Received: 24 September 2016 | Accepted: 17 March 2018
DOI: 10.1002/fut.21923

RESEARCH ARTICLE

WILEY FUTURES MARKETS

# Modeling temperature behaviors: Application to weather derivative valuation

**Jr-Wei Huang**[1,2] | **Sharon S. Yang**[3,4] | **Chuang-Chang Chang**[3]

[1] Department of Insurance, Hubei University of Economics, Wuchang, Wuhan, Hubei Province, China

[2] Institute for Development of Cross-strait Small and Medium Enterprises, Hubei University of Economics, Wuchang, Wuhan, Hubei Province, China

[3] Department of Finance, National Central University, Jhongli City, Taoyuan County, Taiwan, Republic of China

[4] Risk and Insurance Research Center, College of Commerce, National Chengchi University, Wenshan District, Taipei City, Taiwan, Republic of China

**Correspondence**
Sharon S. Yang, Department of Finance, National Central University, No. 300, Jhongda Rd., Jhongli City, Taoyuan County 32001,Taiwan, Republic of China.
Email: syang@ncu.edu.tw

This article investigates temperature behavior to develop a temperature model. The proposed ARFIMA Seasonal GARCH model that allows for long memory effects and other important temperature properties provides better goodness of fits and forecasting accuracy using daily average temperatures in six U.S. cities. The effect of temperature behavior on pricing temperature derivatives is analyzed. We propose an equilibrium option pricing framework for HDD and CDD forward and option contracts under the ARFIMA Seasonal GARCH model. The investigation of temperature properties and the valuation framework in this study contributes to the development of a standardized temperature model for weather derivative markets.

**KEYWORDS**
equilibrium pricing, long memory, temperature derivatives

**JEL CLASSIFICATION**
C4, C5

## 1 | INTRODUCTION

Weather has an important influence on various industries, including power, entertainment, agriculture, retail, transportation, and construction. Worldwide climate changes and abnormal weather have led to significant losses (Impact Forecasting, 2013; IPCC, 2008; Lobell et al., 2007). Recent statistics show that in 2013 the United States suffered economic losses of $17.22 billion due to severe weather; flooding in central Europe during summer months caused economic losses of $22 billion. Then, drought in China between January and August caused losses estimated at $10 billion.[1] Thus, there is a strong need to manage weather risk globally.

The introduction of weather derivatives in the capital market in turn has attracted great attention as a potential tool for hedging weather risks. Weather derivatives are financial contracts that allow entities to hedge against fluctuations in the weather. The first weather derivative, issued in 1997, traded on the temperature in the Over the Counter (OTC) market; today the largest weather derivative market is the Chicago Mercantile Exchange (CME). The latter comprises four location-based subgroups: the United States and Canada, Europe, Japan, and Australia.[2] Approximately 82% of the contracts refer to the United States and Canada market; Europe and Asia represent 11 and 7%, respectively (Brockett et al., 2005). In the former, weather derivatives are

[1]These statistics come from the Impact Forecasting November 2013 Global Catastrophe Recap.

[2]The locations of focal locations are Atlanta, Chicago, Cincinnati, New York, Dallas, Philadelphia, Portland, Tucson, Des Moines, Las Vegas, Boston Houston, Kansas City, Minneapolis, Sacramento, Detroit, Salt Lake City, Baltimore, Colorado, Springs, Jacksonville, Little Rock, Los Angeles, Raleigh, Durham, Washington D.C in United Sates; Calgary, Edmonton, Montreal, Toronto, Vancouver, Winnipeg in Canada; London, Paris, Amsterdam, Berlin, Essen, Stockholm, Barcelona, Rome, Madrid, Oslo-Blindern, Prague in Europe; Tokyo, Osaka, Hiroshima in Japan; Bankstown, Brisbane Aero, Melbourne in Australia.

written by banks, insurance companies, brokers, hedge funds, and other financial companies, tailored to specific end-user. In practice, these OTC contracts can be written for any location or group of locations and for any measurable weather index.

Because of the variability of weather risk, weather derivatives have been structured to cover almost any type of weather variable: temperature, rainfall, snowfall, wind speed, and humidity, for example. According to the recent survey of the weather derivatives market by Weather Risk Management Association (WRMA, 2011a), the CME where weather contracts are largely dominated by temperature-based index has shown that weather risk contracts account for 98%. In addition, weather derivative deals can be structured to refer to maximum, minimum, or daily average temperatures. For example, heating degree days (HDD) and cooling degree days (CDD), defined on the basis of daily average temperatures, are two common derivatives. A company can buy a CDD during the summer or HDD for winter to hedge weather risk. The energy sector is the primary user of weather derivatives (Alaton et al., 2002; Cao & Wei, 2004), though abnormal climates have led to steady growth in the market too. According to the WRMA (2011b) survey report, the weather derivatives market grew by 20% and the total notional value for OTC traded contracts rose to $2.4 billion in 2010–2011, while the overall market grew to $11.8 billion. Weather derivatives thus have gained popularity as tools to manage weather risk.

Even as weather derivatives become more important, no standardized model exists to capture weather dynamics, nor is there any effective valuation method for weather derivatives. For example, several considerations make pricing temperature derivatives more difficult than pricing traditional derivatives (Alaton et al., 2002; Brody et al., 2002; Campbell & Diebold, 2005; Cao & Wei, 2004; Groll et al., 2016; Hardle & Lopez Cabrera, 2012; Huang et al., 2008; Zapranis & Alexandridis, 2009). First, modeling underlying temperature indices is essential to price derivatives but also is challenging, because temperature is highly localized and consists of different features. Second, underlying temperature indices are not tradable and cannot be derived from a no-arbitrage condition, because it is not possible to replicate the payoff of a given contingent claim by a controlled portfolio of basic securities. Third, the liquidity of temperature derivative markets has improved, but they still are not as complete as traditional derivative markets. In turn, we cannot apply a classic Black–Scholes–Merton methodology. Instead, we confront the challenge of developing a temperature forecasting model that can be integrated into an options pricing framework, while also providing accurate estimates and forecasts.

To date, a variety of temperature behaviors have been addressed and the corresponding temperature model is proposed to govern its temperature behavior. Alaton et al. (2002) construct a temperature model that accounts for global warming, seasonality, and mean reversion, and then they derive the closed-form pricing formula for the weather derivative. Huang et al. (2008) extend their work to consider volatility clustering and incorporate a GARCH process with temperature. For both HDD and CDD, the call price is higher with ARCH effects variance than fixed variance. In addition, Cao and Wei (2004) model the dynamics of temperature by considering seasonal variation, mean reversion, volatility clustering, a larger variation in daily temperature in winter than in summer, and global warming. Campbell and Diebold (2005) time-series approach captures and forecasts daily average temperature features, in line with Cao and Wei (2004), but also considers both the conditional mean and conditional variance in daily temperature behavior, constructing a future distribution of underlying temperature indices. Benth and Saltyte-Benth (2007) propose an Ornstein–Uhlenbech process with seasonal volatility to model the time dynamics of daily average temperatures and pricing HDD and CDD futures and options. They show that HDD futures curve gives higher prices when taking into account the seasonal volatility of temperature compared with a constant volatility. Thus prior literature denotes the temperature properties of global warming, seasonality, mean reversion, volatility clustering, and seasonal cyclical in volatility to model temperature.

Another important feature is that temperature variability may exert a long memory effect (Benth, 2003; Brody et al., 2002; Caballero et al., 2002; Syroka & Toumi, 2001; Tsonis et al., 1999). This long memory arises from the presence of positive long-range correlations or persistence in temperature data. If an anomaly with a particular sign exists in the past, it likely persists in the future. Existing research suggests two ways to identify the long memory effects for temperature. First, Syroka and Toumi (2001) use a simple method to identify the presence of long-range dependence in temperature data. Brody et al. (2002) apply their method to test for long memory, but whereas Syroka and Toumi (2001) rely on fractional Brownian motion to model temperature dynamics, Brody et al. (2002) propose a fractional Ornstein–Uhlenbeck process to price HDD and CDD contracts using partial differentials. Second, Caballero et al. (2002) use an econometric approach, focusing on long memory effects with conditional mean dynamics of temperature and employing autoregressive fractionally integrated moving average (ARFIMA) models to reflect temperature dynamics. They find that the long memory model from ARFIMA provides more accurate pricing results than the short memory version. Benth (2003) also considers the effect of long memory in temperature evolution, together with a mean reversion toward seasonal variation, though without any empirical test. With the assumption that temperature follows a fractional Ornstein–Uhlenbeck process, he uses an arbitrage-free method to price dynamics for claims on temperature. Schiller et al. (2012) proposed the splines model to separate the daily temperature data into trend and seasonality component. Further, they model the

residuals with an Autoregressive on Moving Average (AROMA) process previously proposed by Jewson and Caballero (2003) to capture the long memory feature.

Overall, long memory for temperature dynamics clearly has an important influence on temperature models. If a temperature model fails to capture this long memory, it significantly underprices weather options (Caballero et al., 2002). Most studies focus on examining long memory and employ rather simple models to govern temperature dynamics. Because pricing temperature derivatives depends on the expected evolution of the temperature variable, other temperature behaviors, such as global warming, seasonality, mean reversion, seasonal cyclical in volatility (Cao & Wei, 2004), or volatility clustering (Campbell & Diebold, 2005; Huang et al., 2008), also may be important. Extending existing literature on long memory, taking these factors into consideration thus is critical for modeling temperature dynamics accurately. Thus, Jewson and Brix (2005) also conclude that the risk with daily modeling is that small misspecification in the models can lead to large mispricing of the temperature contract.

In response, we build a complete model of temperature processes that can capture long memory and other important temperature properties. In our ARFIMA–SGARCH model, temperature dynamics include not only conditional mean dynamics, with contributions from global warming, seasonal and cyclical components, and long memory, but also conditional volatility dynamics and the contributions of both seasonal and cyclical components. We attempt to define the impact of different temperature properties using real data. In the empirical analysis, we thus examine the performance of the proposed ARFIMA–SGARCH model and compare with other temperature models introduced in previous literature (Alaton et al., 2002; Benth & Saltyte-Benth, 2007; Campbell & Diebold, 2005; Huang et al., 2008), evaluating both their fit and forecasting performance for different temperature properties. We also use econometric tools to detect the presence of long memory in temperature. To measure model risk, we investigate the effect of temperature properties on temperature derivatives numerically. Thus we deal with the valuation problem for temperature derivatives in the incomplete market, using an equilibrium option pricing method. Whereas Cao and Wei (2004) apply an extended version of Lucas (1978) equilibrium pricing model to price HDD and CDD contracts—which avoids direct estimation of the market price of weather risk and bases the pricing instead on the stochastic process of the weather index, an aggregated dividend, and assumptions about the utility function of a representative investor—we also extend the equilibrium option pricing method to price the HDD and CDD contracts under the ARFIMA–SGARCH model.

For our empirical study, we rely on United States daily average temperature data from six measurement stations (Atlanta, Chicago, Dallas, New York, Philadelphia, and Las Vegas). We extend studies that demonstrate long memory across regions (Brody et al., 2002; Caballero et al., 2002; Syroka & Toumi, 2001), such as central England, the United States, and El Nino regions, by investigating the temperature dynamics in these U.S. cities separately. To assess model fit and temperature behaviors, we divide the full sample into in- and out-of-sample periods in our model evaluation. The empirical study shows that the proposed ARFIMA–SGARCH model leads to the best fit for both in-sample fit and out-of-sample forecasts. Finally, we find significant model risk in pricing weather derivatives when we ignore temperature properties will lead to large mispricing of the temperature contract. The empirical findings are consistent with Jewson and Brix (2005).

This study provides a general valuation model for temperature properties that not only allows for the long memory effect but also recognizes the major properties needed to price temperature derivatives. We contribute to existing literature in four main ways. First, we verify important temperature properties with real data. Understanding these properties can help the development of a standardized temperature model for the weather derivative market. Second, the ARFIMA–SGARCH model is first proposed to capture temperature uncertainty, according to model performance, by comparing a range of temperature models. Thus we can capture major temperature behavior. Third, we obtain an equilibrium framework for dealing with the HDD forward and option contracts in an incomplete market under the ARFIMA–SGARCH model. This valuation framework can encourage the use of temperature derivatives to manage weather risk. Forth, in line with Jewson and Brix (2005) finding, we also find that model risk is very significant, ranging from 3.12 to 20.14% and 4.76 to 49.97% for forward and option contracts, respectively. And, the most significant model risk stems from ignoring the cyclical components in mean; the least significant involves ignoring global warming in this study.

We organize the remainder of this paper as follows: Section 2 we provide an in-depth analysis of the econometrics of weather temperature data. In section 3 we construct our ARFIMA–SGARCH model and present the empirical analysis of in-sample and out-of-sample performance, in comparison with other weather temperature models. We explain the pricing of HDD forward and option contracts under Cao and Wei (2004) framework in section 4 before concluding with a discussion.

## 2 | TEMPERATURE PROPERTIES

To capture the future dynamic effects of weather uncertainty on temperature, we conducted an empirical study to examine the pattern of variation in the proposed temperature model. For comparisons, we consider temperatures in six U.S. cities: Atlanta,

**TABLE 1** Descriptive statistics

| | Atlanta | Chicago | Dallas | New York | Philadelphia | Las Vegas |
|---|---|---|---|---|---|---|
| Observations | 6,966 | 6,966 | 6,966 | 6,966 | 6,966 | 6,966 |
| Mean | 62.360 | 50.624 | 66.847 | 55.846 | 56.306 | 69.715 |
| Maximum | 13.700 | 92.300 | 98.200 | 93.700 | 92.900 | 105.500 |
| Minimum | 92.800 | −12.900 | 16.100 | 8.500 | 9.500 | 30.400 |
| Std. Dev. | 14.740 | 19.656 | 16.230 | 17.014 | 17.192 | 17.359 |
| Skewness | −0.417[a] | −0.250[a] | −0.354[a] | −0.135[a] | −0.178[a] | 0.049 |
| Excess kurtosis | −0.777[a] | −0.844[a] | −0.793[a] | −0.942[a] | −0.998[a] | −1.271[a] |
| Jarque–Bera | 377.65[a] | 280.01[a] | 328.39[a] | 279.36[a] | 326.32[a] | 472.20[a] |

Skewness and excess kurtosis statistics include a test of the null hypotheses, where each is zero (population values if the series is i.i.d. normal). The Jarque-Bera statistic tests for normality with a combination of skewness and kurtosis measures.

[a]Significant at the 1% level.

Chicago, Dallas, New York, Philadelphia, and Las Vegas, from January 1, 1995, through January 31, 2014, which produced 6,966 observations per station.[3] The primary data source is the National Climate Data Center, a subsidiary of the National Oceanic Atmospheric Administration; temperatures are measured in degrees Fahrenheit.

## 2.1 | Statistical analysis of temperature data

Given a specific weather station, we let $W_t^{\max}$ and $W_t^{\min}$ denote the maximal and minimal temperatures (in degrees Fahrenheit) measured at time $t$. We define the daily average temperature as

$$W_t = \frac{W_t^{\max} + W_t^{\min}}{2} \tag{1}$$

To understand the temperature pattern in each city, we first provide summary statistics of the daily average temperatures for these cities in Table 1 and plot their trends over nearly 20 years in Figure 1. The temperatures clearly indicate four distinct seasons. The daily average temperature moves repeatedly and regularly though periods of higher (summer) and lower (winter) temperatures. These characteristics justify the inclusion of seasonality in the model. The daily average temperature also varies across different ranges for each station. For example, the maximum daily average temperature is 105.5°F and the minimum daily average temperature is 30.4°F in Las Vegas; these values in Chicago are, respectively, 92.3°F and −12.9°F. The summary statistics thus show that the average temperature for each station is highly localized. In addition, we find evidence of global warming in each station, in that temperatures have oscillated but increased over time. The distributions of daily average temperatures are in Figure 2. According to the shape of the density function, the distribution of daily average temperature is platykurtic and negatively skewed, except in Las Vegas. The densities of temperature are either bimodal or nearly so, with peaks of cool and warm temperatures, consistent with Neese (1994) finding of skewness and bimodality in maximum daily U.S. temperatures. According to the volatility of daily average temperatures in Figure 3, there is a clear seasonal pattern, such that temperature variations in the winter are larger than those in the summer, consistent with Cao and Wei (2004) results.

## 2.2 | Testing long memory effects for temperature

We first examine the long memory effect using temperatures in Atlanta, Chicago, Dallas, New York, Philadelphia, and Las Vegas. Fractional integration (or fractional differencing), as devised by Granger and Joyeux (1980) and Hosking (1981), provides a means to model a process with long memory. Granger and Joyeux (1980) show that the long memory process is

[3]Cao and Wei (2004) use daily temperature data from Atlanta, Chicago, Dallas, New York, and Philadelphia to derive a temperature model. Campbell and Diebold (2005) model daily average temperatures for Atlanta, Chicago, Las Vegas, and Philadelphia. Neither investigates long memory effects. For comparisons, we included these cities in our analysis as well.

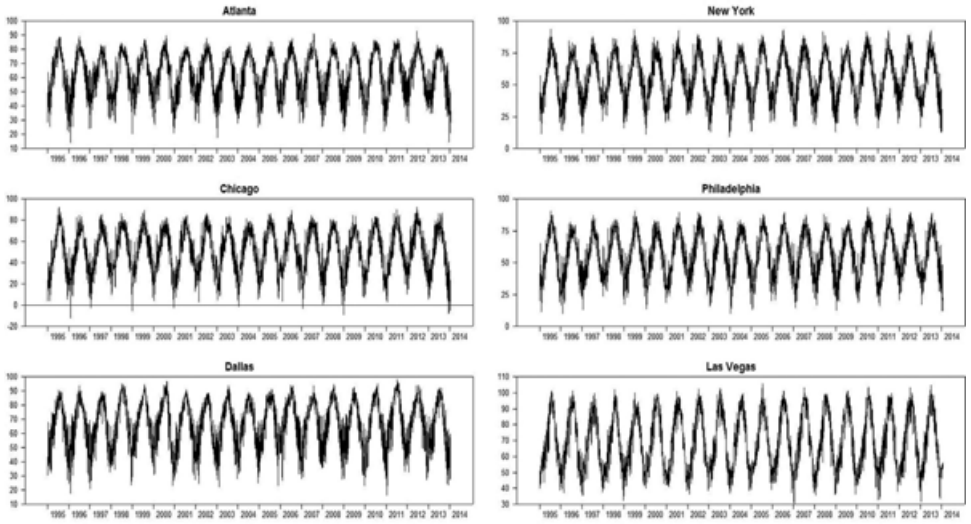


**FIGURE 1** Time series plots of daily average temperatures, January 1, 1995–January 31, 2014

stationary and can be characterized by an autocorrelation function (ACF) that decays slowly at a hyperbolic rate; the ACF for a short memory process instead decays at an exponential rate. Short memory can be represented by the ARMA process. Figure 4 contains the ACF values for Atlanta, Chicago, Dallas, New York, Philadelphia, and Las Vegas temperatures; this ACF is very slow and looks closer to hyperbolic than exponential. That is, the temperature process appears to include long memory effects. We also use econometric approaches to detect their presence, namely, those introduced by Hurst (1951), Lo (1991), and Geweke and Porter-Hudak (1983). These long memory methods have been used widely to analyze with stock returns and economic time series (Aydogan & Booth, 1988; Cheung, 1993; Cheung & Lai, 1995; Chow et al., 1995; Greene & Fielitz 1977; Jacobsen, 1996; Lo, 1991); most evidence suggests the absence of long memory in stock returns but its presence in foreign exchange rate series. Thus, we employ three methods to detect the long memory property of temperature data, as we describe in Appendix A.

Using 6,966 observations from each station, reflecting the daily average temperature from January 1995 through January 2014, we first check for stationarity, because a non-stationary series behaves like a long memory process and would lead to a biased result. To ensure temperature series are stationary, we apply both augmented Dickey and Fuller (1981) (ADF; 1981) and Phillips and Perron (1988) tests. Panels A and B in Table 2 contain the results for the unit root test and long memory test, respectively. In Panel A, the tests both reject the null unit root hypothesis; the temperature series in Atlanta, Chicago, Dallas, New York, Philadelphia, and Las Vegas are stationary. The results of the long

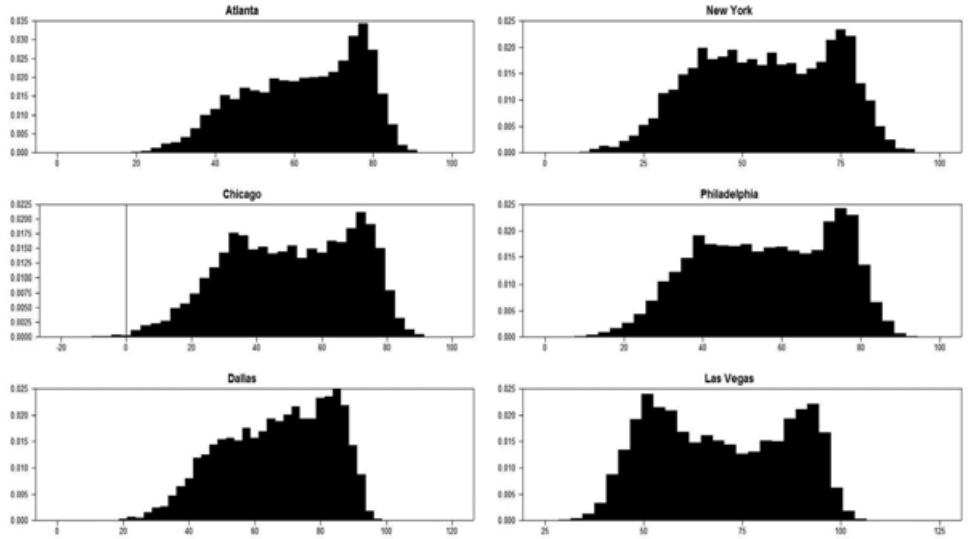


**FIGURE 2** Histograms of daily average temperatures, January 1, 1995–January 31, 2014

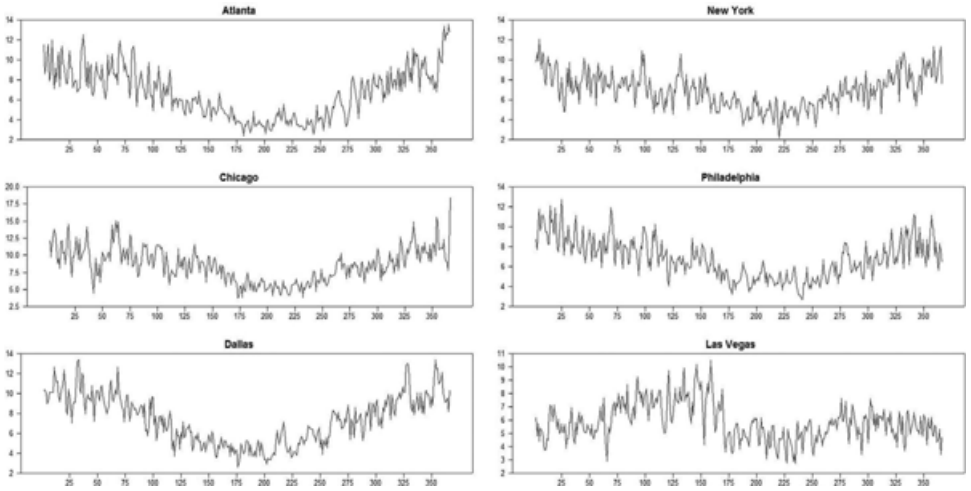


**FIGURE 3** Volatility of daily average temperatures. This graph shows the standard deviation for each of the 365 calendar days, with the standard deviation calculated from January 1, 1995 to January 31, 2014

memory test in Panel B confirm the presence of long memory effects for daily average temperatures in each station (Geweke & Porter-Hudak, 1983; Hurst, 1951; Lo, 1991). Furthermore, the empirical results are consistent with Syroka and Toumi (2001), Caballero et al. (2002), and Brody et al. (2002), indicating long memory across different regions. Based on the existing literature and empirical observation, several features should be considered for daily average temperature model:

**1.** It moves around a seasonal mean.
**2.** It should incorporate cyclical components in the mean (i.e., it appear to have autoregressive in mean).
**3.** It is affected by global warming and urban effects.
**4.** Its volatility is higher in the winter than in summer.
**5.** Volatility clustering should exist in temperature (i.e., it appear to have autoregressive changes).
**6.** The long memory effect should appear for temperature.

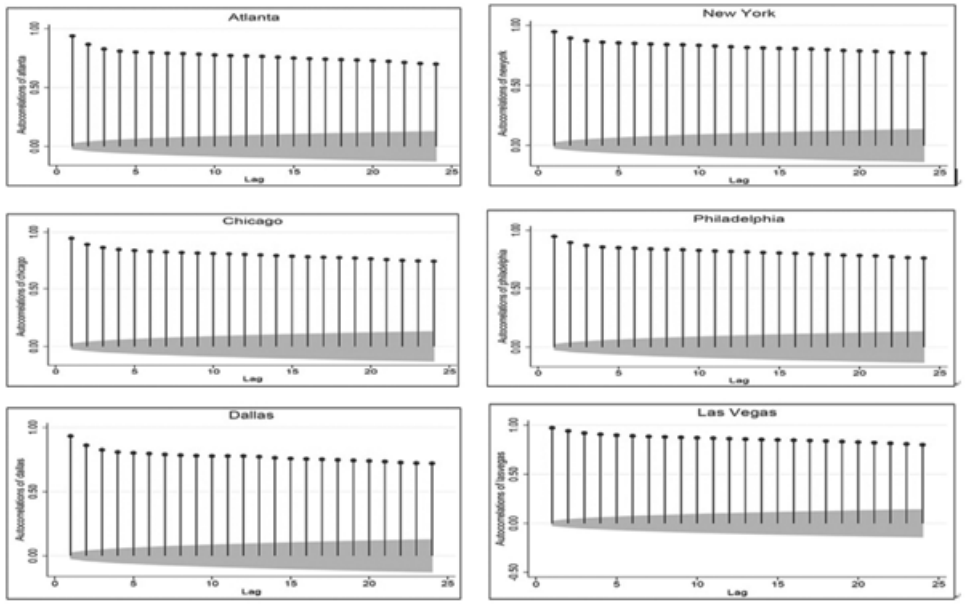


**FIGURE 4** ACF for daily average temperatures. Gray-shaded areas indicate the 95% confidence intervals around the observed estimate

**TABLE 2** Unit root and long memory tests for daily average temperatures

| **Panel A: Unit root test** | | | |
|---|---|---|---|
| | **Augmented Dickey–Fuller test** | | **Phillips–Perron test** |
| Atlanta | −71.638[a] | | −13.018[a] |
| Chicago | −68.623[a] | | −11.763[a] |
| Dallas | −68.030[a] | | −13.358[a] |
| New York | −57.929[a] | | −11.336[a] |
| Philadelphia | −55.702[a] | | −11.311[a] |
| Las Vegas | −51.454[a] | | −8.818[a] |
| **Panel B: Long memory test** | | | |
| | **Hurst (1951)** | **Lo (1991)** | **Geweke and Porter-Hudak (1983)** |
| Atlanta | $H = 0.712$ | $V = 2.970$[b] | $\hat{d}$ =0.159[b] |
| Chicago | $H = 0.740$ | $V = 3.284$[b] | $\hat{d}$ =0.190[b] |
| Dallas | H = 0.705 | $V = 3.269$[b] | $\hat{d}$ =0.212[b] |
| New York | $H = 0.749$ | $V = 2.959$[b] | $\hat{d}$ =0.180[b] |
| Philadelphia | $H = 0.720$ | $V = 3.188$[b] | $\hat{d}$ =0.147[b] |
| Las Vegas | $H = 0.687$ | $V = 2.944$[b] | $\hat{d}$ =0.130[b] |

In Panel A, the unit root test under the null hypothesis is I (1) series. In Panel B, the Hurst (1951) show that if $0.5 < H < 1$, the process presents a long memory effect; the critical values of Lo (1991)'s test at the 5% level is 1.747; the critical values of GPH(1983)'s test at 5% level is 1.96.

[a]Significant at 1%.

[b]Significant at 5%.

# 3 | MODELING TEMPERATURE TIME SERIES

## 3.1 | Temperature process using ARFIMA–SGARCH model

After verifying the presence of long memory in Atlanta, Chicago, Dallas, New York, Philadelphia, and Las Vegas temperatures, we extend the well-developed temperature model proposed by Campbell and Diebold (2005) to allow for a long memory effect. Our new dynamic model for temperature evolution is the ARFIMA Seasonal GARCH (ARFIMA–SGARCH) model, which focuses on conditional mean dynamics, with contributions from global warming, seasonal and cyclical components, and long memory, while also allowing for conditional volatility dynamics, with contributions from both seasonal and cyclical components.

Two specifications are required to develop the ARFIMA–SGARCH model: the conditional mean and the conditional variance. The daily average temperature model is

$$W_t = u_t + \varepsilon_t, \tag{2}$$

where $u_t$ affects the mean of the daily average temperature, and $\varepsilon_t$ represents the stochastic component of the daily average temperature. The deterministic function of $u_t$ takes the following structure:

$$u_t = \alpha_0 + \alpha_1 t + \sum_{j=1}^{P}\left(\delta_j \cos\left(\frac{2jt\pi}{365}\right) + \gamma_l \sin\left(\frac{2jt\pi}{365}\right)\right), \tag{3}$$

where $\alpha_1$ is the global warming factor, and $\delta_j$ and $\gamma_l$ capture the seasonal cyclical mean. The stochastic component of the daily average temperature $\varepsilon_t$ follows a ARFIMA–SGARCH model,

$$\Phi(L)(1-L)^d \varepsilon_t = \Theta(L)\eta_t, \tag{4}$$

$$\eta_t | F_{t-1} \sim N\left(0, h_t^2\right), \text{ and} \tag{5}$$

$$h_t^2 = \sum_{q=1}^{H}\left(\varsigma_q \cos\left(\frac{2qt\pi}{365}\right) + \varphi_q \sin\left(\frac{2qt\pi}{365}\right)\right) + \sum_{j=1}^{Q}\omega_j \eta_{t-j}^2 + \sum_{i=1}^{E}\beta_i h_{t-i}^2, \tag{6}$$

such that in Equation (4), we capture cyclical mean components using autoregressive lags. Thus $\Phi(L) = 1 - \sum_{i=1}^{p} \kappa_i L^i$ and $\Theta(L) = 1 + \sum_{i=1}^{q} \nu_i L^i$ are the AR and MA polynomials in the lag operator $L$ (i.e., $L^m \varepsilon_t = \varepsilon_{t-m}$) with orders $p$ and $q$, respectively. Furthermore, $d$ is the fraction differencing parameter, which can take any non-integer values. The innovation term ($\eta_t$) in Equation (5) is conditional on the information set at time $t-1$ (denoted by $F_{t-1}$), following a normal distribution with mean zero and variance $h_t^2$. The factors of $\varsigma_q, \varphi_q, \beta_i$ characterize $h_t^2$ in Equation (6), with contributions from both the seasonal cycle in volatility and volatility clustering components.

## 3.2 | Parameter estimates in ARFIMA–SGARCH model

To understand the effect of temperature behavior, we employ real temperature data and estimate the parameters for the proposed ARFIMA–SGARCH model using Atlanta, Chicago, Dallas, New York, Philadelphia, and Las Vegas daily average temperatures, as described in section 2.1. For the ARFIMA–SGARCH model, however, no closed-form expression for the exact likelihood function is available. Therefore, we employ the conditional sum of squares (CSS) estimator:

$$\widehat{\Xi} := \arg\max_{\Xi} L(\Xi) \tag{7}$$

where

$$\begin{aligned} &\Xi := (u_1, \Xi_1)', u_1 := (\alpha_0, \alpha_1, \delta_1, \cdots, \delta_P, \gamma_1, \cdots, \gamma_P), \\ &\Xi_1 := \left(\kappa_1, \cdots, \kappa_p, \nu_1, \cdots, \nu_q, d, \varsigma_1, \cdots, \varsigma_H, \varphi_1, \cdots, \varphi_{\mathrm{H}}, \omega_1, \cdots, \omega_{\mathrm{Q}}, \beta_1, \cdots, \beta_{\mathrm{E}}\right) \end{aligned} \tag{8}$$

and

$$L(\Xi) := -\frac{1}{2} \sum_{t=1}^{T} \left( \ln h_t^2(\Xi) + M_t(\Xi)^2 \right) \tag{9}$$

$$\begin{aligned} M_t(\Xi) &:= \eta_t(\Xi) / \sqrt{h_t^2(\Xi)} \\ \eta_t(\Xi) &:= \Theta(L)^{-1} \Phi(L) (1-L)^d (W_t - u_t(\Xi)) \\ u_t(\Xi) &= \alpha_0(\Xi) + \alpha_1 t(\Xi) + \sum_{j=1}^{P} \left( \delta_j \cos\left(\frac{2jt\pi}{365}\right)(\Xi) + \gamma_l \sin\left(\frac{2jt\pi}{365}\right)(\Xi) \right) \\ h_t^2(\Xi) &= \sum_{q=1}^{H} \left( \varsigma_q \cos\left(\frac{2qt\pi}{365}\right)(\Xi) + \varphi_q \sin\left(\frac{2qt\pi}{365}\right)(\Xi) \right) + \sum_{j=1}^{Q} \omega_j \eta_{t-j}^2(\Xi) + \sum_{i=1}^{E} \beta_i h_{t-i}^2(\Xi) \end{aligned} \tag{10}$$

The asymptotic behavior of this estimate was formally established by Ling and Li (1997). Thus, we use the Akaike and Bayesian information criteria to select the lag structure ($P = 1$, $H = 1$, $Q = 1$, $E = 1$, $p = 3$, $q = 0$) of the ARFIMA–SGARCH model.[4]

Table 3 presents the estimation results. We discover some important temperature behavior from the conditional mean Equations (3) and (4) and the conditional variance Equation (6). First, the average temperature in each station displays statistically significant, increasing global warming in daily average temperatures. This result may be associated with both urbanization and global warming effects. Second, conditional mean dynamics display strong cyclical persistence; $\kappa_i$ are statistically significant. Third, the conditional mean dynamics display both statistically and economically important seasonality, consistent with Figure 1. Fourth, the fraction differencing parameter $0 < \hat{d} < 0.5$ is significant, which implies that the temperature in each station has a long memory effect, consistent with Caballero et al. (2002), who find a long memory effect for both central England and U.S. daily temperatures. However, Caballero et al. (2002) did not incorporate uncovers two interesting findings regarding the effect in the conditional variance (Equation (6)). Specifically, volatility appears seasonal, such that the amplitude of the residual fluctuation varies over the course of each year, widening in winter and narrowing in summer. The conditional variance also displays strong cyclical persistence, so the coefficient of conditional variance is significantly positive. In contrast with previous literature, the proposed ARFIMA–SGARCH model can capture six dynamics in the temperature time evaluation.

[4]AIC = − 2/T ln (likelihood) + 2/T × (number of parameters) (Akaike, 1973). BIC = − 2/T ln (likelihood) + (]number of parameters] × ln [T])/T.

**TABLE 3** Parameter estimated for daily average temperature from January 1, 1995 to January 31, 2014[a]

| Parameter | Atlanta | Chicago | Dallas | New York | Philadelphia | Las Vegas |
|---|---|---|---|---|---|---|
| $\alpha_0$ | 7.4604[c] | 5.8893[c] | 6.3044[c] | 7.3922[c] | 8.4178[c] | 7.9820[c] |
| | (0.2395) | (0.2105) | (0.2154) | (0.2297) | (0.2502) | (0.2677) |
| $\alpha_1$ | 4e-4[c] | 4e-4[c] | 4e-4[c] | 4e-4[c] | 4e-4[c] | 4e-4[c] |
| | (2e-5) | (3e-5) | (2e-5) | (3e-5) | (3e-5) | (2e-5) |
| $\delta_1$ | −3.5809[c] | −5.0918[c] | −3.7575[c] | −5.0997[c] | −5.2731[c] | −4.0488[c] |
| | (0.1247) | (0.1648) | (0.1285) | (0.1555) | (0.1608) | (0.1426) |
| $\gamma_1$ | 0.1771[c] | 0.4085[c] | 0.6332[c] | 0.3911[c] | −0.8680[c] | −0.3490[c] |
| | (0.0682) | (0.0917) | (0.0788) | (0.0826) | (0.0899) | (0.0652) |
| $\kappa_1$ | 0.8106[c] | 0.7074[c] | 0.7121[c] | 0.6715[c] | 0.7293[c] | 0.8635[c] |
| | (0.0129) | (0.0123) | (0.0126) | (0.0122) | (0.0122) | (0.0122) |
| $\kappa_2$ | −0.2782[c] | −0.2273[c] | −0.2553[c] | −0.2321[c] | −0.2416[c] | −0.2303[c] |
| | (0.0156) | (0.0146) | (0.0149) | (0.0143) | (0.0144) | (0.0121) |
| $\kappa_3$ | 0.0859[c] | 0.0680[c] | 0.0943[c] | 0.0759[c] | 0.0725[c] | 0.0696[c] |
| | (0.0122) | (0.0123) | (0.0126) | (0.0120) | (0.0122) | (9e-5) |
| $\varsigma_1$ | 0.0716[c] | 0.1410[c] | 0.0235[b] | 0.0889[c] | 0.1339[c] | 0.0454[c] |
| | (0.0080) | (0.0140) | (0.0095) | (0.0105) | (0.0098) | (0.0075) |
| $\phi_1$ | −0.2029[c] | −0.2726[c] | −0.2791[c] | −0.1821[c] | −0.1901[c] | −0.0085 |
| | (0.0104) | (0.0170) | (0.0127) | (0.0115) | (0.0114) | (0.0084) |
| $\omega_1$ | 0.0264[c] | 0.0266[c] | 0.0313[c] | 0.0181[c] | 0.0215[c] | 0.0217[c] |
| | (0.0028) | (0.0037) | (0.0027) | (0.0031) | (0.0028) | (0.0028) |
| $\beta_1$ | 0.9735[c] | 0.9733[c] | 0.9686[c] | 0.9818[c] | 0.9784[c] | 0.9782[c] |
| | (0.0028) | (0.0037) | (0.0027) | (0.0031) | (0.0028) | (0.0028) |
| $d$ | 0.1585[b] | 0.1907[b] | 0.2122[b] | 0.1796[b] | 0.1474[b] | 0.1299[b] |
| | (0.0799) | (0.0691) | (0.0741) | (0.0859) | (0.0731) | (0.0788) |
| AIC | 39,630.37 | 43,581.15 | 41,409.62 | 41,732.78 | 41,464.28 | 38,075.38 |
| BIC | 39,712.55 | 43,663.33 | 41,491.80 | 41,814.96 | 41,546.46 | 38,157.56 |
| Log-likelihood | −19,803.18 | −21,778.57 | −20,692.81 | −20,854.39 | −20,720.14 | −19,025.69 |

Standard errors are in parentheses.

[a]We used the Akaike and Bayesian information criteria to select the lag structure ($P = 1, H = 1, Q = 1, E = 1, p = 3, q = 0$) of the ARFIMA–SGARCH model.

[b]Significant at 5%.

[c]Significant at 1%.

## 3.3 | Comparison of goodness-of-fit of different temperature models

Different temperature models display different temperature behaviors. To verify the temperature behaviors in the modeling, we investigate the model fit of different temperature models which pose different temperature behaviors, using real data. We then compare six temperature models studied in the literature with the proposed ARFIMA–SGARCH model which are: Model 1 by Alaton et al. (2002), Model 2 by Huang et al. (2008), Model 3 by Campbell and Diebold (2005), Model 4 by Campbell and Diebold (2005) but without controlling for the seasonal effect in the conditional volatility, Model 5 by Benth and Saltyte-Benth (2007), Model 6 following the ARFIMA–GARCH process, and Model 7 as the proposed ARFIMA–SGARCH model. The stochastic processes are described in Appendix B. For comparison purposes, we summarize the temperature properties characterized by these seven models in Table 4. These temperature models address multiple temperature properties: seasonal cycles in the mean, global warming, cyclical components in the mean, long memory seasonal cycles in volatility, and volatility clustering. Model 1 (Alaton et al., 2002) considers only two properties, global warming and seasonal effect in mean levels; Model 2 (Huang et al., 2008) considers global warming and seasonal effects in the mean and volatility clustering; Model 3 (Campbell & Diebold, 2005) includes five properties: the seasonal cycle in mean, global warming, cyclical components in mean, seasonal cycles in volatility, and volatility clustering; Model 5 (Benth & Saltyte-Benth, 2007) consider three properties, global warming and seasonal effect in mean and volatility levels. The proposed Model 7 includes six properties.

**TABLE 4** Comparisons of temperature properties in different models

| Temperature Pattern | Model 1 | Model 2 | Model 3 | Model 4 | Model 5 | Model 6 | Model 7 |
|---|---|---|---|---|---|---|---|
| Seasonal cycle in mean | ● | ● | ● | ● | ● | ● | ● |
| Global warming | ● | ● | ● | ● | ● | ● | ● |
| Cyclical components in mean | | | ● | ● | | ● | ● |
| Long memory | | | | | | ● | ● |
| Seasonal cycles in volatility | | | ● | | ● | | ● |
| Volatility clustering | | ● | ● | ● | | ● | ● |

Model 1 Alaton et al. (2002); Model 2 Huang et al. (2008); Model 3 Campbell and Diebold (2005); Model 4 Campbell and Diebold (2005) without controlling for seasonal effects in conditional volatility; Model 5 Benth and Saltyte-Benth (2007); Model 6 ARFIMA–GARCH process; Model 7 ARFIMA–SGARCH model, or Equations (2–6).

To evaluate these models, we perform both in-sample and out-of-sample fits. Temperature data from January 1, 1995–January 31, 2011 represent the in-sample period; the year from February 2, 2011 to January 31, 2014 is the out-of-sample period. Temperature data between 1995 and January 2011 serve to estimate the parameters of the models and thus to generate forecasts for the out-of-sample period. We use log-likelihood and the AIC and BIC information criteria to measure in-sample model performance. The results in Table 5 presents a consistent finding that the ARFIMA–SGARCH (Model 7) offers the best model fit, whereas Model 1 is the worst one in terms of log-likelihood, AIC, and BIC. A simpler model that ignores the cyclical component, long memory in the conditional mean, and seasonal and cyclical components in conditional variance cannot well capture weather dynamics. Models 2 and 5 both perform better than Model 1, so including volatility clustering and seasonal effect in volatility improves model fit. Our comparison of Model 3 with Model 4 or Model 6 with Model 7 reveals that seasonal variation in volatility also improves fit. Finally, the improvements in Models 3 and 7 over Models 4 and 6 show considerable benefits obtained from using long memory models.

Next we compare the performance of the out-of-sample forecast for Models 1–7. The out-of-sample exercise is performed from February 2, 2011- to January 31, 2014. Forecast performance is measured by relative error (RE), unbiased absolute percentage error (UAPE), mean squared percentage error (MSPE), and mean absolute percentage error (MAPE).[5] We follow Papazian and Skiadopoulos (2010) forecasting approach. That is, non-overlapping forecasts are formed for forecast horizon of 1, 5, and 10 days. Table 6 presents the forecasting error results for 1 days forecast horizon. For robustness check, we also consider the forecasting error results for 5 and 10 days forecast horizon in Tables 7 and 8, respectively. Tables 6–8 present three important findings. First, ignoring the cyclical component, long memory in the conditional mean and seasonal and cyclical components in the conditional variance component produce the largest forecasting error. Second, considering seasonal variation in volatility and long memory at the mean decreases the forecasting error. Third, the proposed ARFIMA–SGARCH model provides the best forecasting performance, such that six temperature properties appear critical for modeling the temperature dynamics in each U.S. station.

# 4 | VALUATION FRAMEWORK OF TEMPERATURE DERIVATIVES WITH THE ARFIMA–SGARCH MODEL

## 4.1 | Equilibrium option pricing approach for temperature derivatives

Temperature is not a tradable asset, so a traditional, no arbitrage, risk-neutral valuation approach cannot be applied to price temperature derivatives (HDDs and CDDs). We use an equilibrium option pricing method, which extends the approach adopted by Cao and Wei (2004), who apply an extended version of Lucas (1978) equilibrium pricing model, which avoids a direct estimation of the market price of weather risk. Pricing instead is based on a stochastic process of the weather index, an aggregated dividend, and assumptions about the utility function for a representative investor. In other words, their equilibrium pricing model contains a joint process of temperature and aggregated dividend.

According to Lucas (1978) pre-exchange economy, fundamental uncertainties are driven by the aggregate dividend $\theta_t$ and a state variable that represents the weather condition of temperature $W_t$. Aggregative dividends constitute the aggregate output. For a representative investor, the equilibrium conditions imply total consumption is equal to the aggregate dividend; the time $t$

[5] The measurement can be defined as $\mathrm{RE} = \frac{1}{N}\sum_{t=1}^{N} W_t - \hat{W}_t / W_t$, $\mathrm{UAPE} = \frac{1}{N}\sum_{t=1}^{N}\left| W_t - \hat{W}_t / \left(W_t + \hat{W}_t / 2\right)\right|$, $\mathrm{MSPE} = \frac{1}{N}\sum_{t=1}^{N}\left(W_t - \hat{W}_t / W_t\right)^2$, and $\mathrm{MAPE} = \frac{1}{N}\sum_{t=1}^{N}\left|\frac{W_t - \hat{W}_t}{W_t}\right|$, where $W_t$ is the actual value of the daily average temperature, $\hat{W}_t$ is the forecast value of the daily average temperature, and $N$ is the number of observations.

**TABLE 5** Fitting performance for different models, Janiary 1, 1995–January 31, 2011

| City | Model | Log-Likelihood | AIC | BIC |
|---|---|---|---|---|
| Atlanta | Model 1 | −19,868.907 | 39,745.814 | 39,772.528 |
| | Model 2 | −19,038.595 | 38,091.190 | 38,137.939 |
| | Model 3 | −16,686.959 | 33,393.919 | 33,460.698 |
| | Model 4 | −16,740.512 | 33,501.024 | 33,567.804 |
| | Model 5 | −19,267.817 | 38,549.634 | 38,596.383 |
| | Model 6 | −16,673.092 | 33,370.184 | 33,450.319 |
| | Model 7 | −16,628.837 | 33,281.675 | 33,361.810 |
| Chicago | Model 1 | −21,084.459 | 42,176.918 | 42,203.631 |
| | Model 2 | −20,309.700 | 40,633.400 | 40,680.149 |
| | Model 3 | −18,332.737 | 36,689.474 | 36,759.280 |
| | Model 4 | −18,336.250 | 36,692.501 | 36,769.609 |
| | Model 5 | −20,744.925 | 41,503.850 | 41,550.599 |
| | Model 6 | −18,331.862 | 36,683.724 | 36,754.679 |
| | Model 7 | −18,325.271 | 36,674.543 | 36,750.504 |
| Dallas | Model 1 | −20,357.808 | 40,723.616 | 40,750.330 |
| | Model 2 | −19,561.967 | 39,137.935 | 39,184.684 |
| | Model 3 | −17,428.983 | 34,877.967 | 34,944.746 |
| | Model 4 | −17,458.359 | 34,936.719 | 35,003.499 |
| | Model 5 | −19,816.759 | 39,647.519 | 39,694.268 |
| | Model 6 | −17,395.061 | 34,814.122 | 34,894.257 |
| | Model 7 | −17,371.606 | 34,767.212 | 34,847.348 |
| New York | Model 1 | −19,862.135 | 39,732.271 | 39,758.985 |
| | Model 2 | −19,281.134 | 38,576.269 | 38,623.018 |
| | Model 3 | −17,627.722 | 35,276.071 | 35,342.850 |
| | Model 4 | −17,628.035 | 35,279.444 | 35,359.579 |
| | Model 5 | −19,662.842 | 39,339.685 | 39,386.435 |
| | Model 6 | −17,615.427 | 35,254.854 | 35,334.990 |
| | Model 7 | −17,593.156 | 35,206.313 | 35,273.093 |
| Philadelphia | Model 1 | −19,883.183 | 39,774.367 | 39,801.081 |
| | Model 2 | −19,227.925 | 38,469.851 | 38,516.601 |
| | Model 3 | −17,497.980 | 35,019.961 | 35,100.096 |
| | Model 4 | −17,522.619 | 35,065.238 | 35,132.018 |
| | Model 5 | −19,582.467 | 39,178.934 | 39,225.683 |
| | Model 6 | −17,479.098 | 34,978.196 | 35,044.976 |
| | Model 7 | −17,466.830 | 34,957.660 | 35,037.795 |
| Las Vegas | Model 1 | −19,121.948 | 38,251.897 | 38,278.611 |
| | Model 2 | −18,272.053 | 36,558.106 | 36,604.855 |
| | Model 3 | −15,985.158 | 31,996.317 | 32,083.128 |
| | Model 4 | −16,007.763 | 32,041.527 | 32,128.339 |
| | Model 5 | −19,038.968 | 38,091.936 | 38,138.685 |
| | Model 6 | −15,960.891 | 31,943.782 | 32,017.238 |
| | Model 7 | −15,891.294 | 31,804.588 | 31,878.044 |

Model 1 Alaton et al. (2002); Model 2 Huang et al. (2008); Model 3 Campbell and Diebold (2005); Model 4 Campbell and Diebold (2005) without controlling for seasonal effects in conditional volatility; Model 5 Benth and Saltyte-Benth (2007); Model 6 ARFIMA–GARCH process; Model 7 ARFIMA–SGARCH model, or Equations (2–6).

**TABLE 6** One-day ahead forecasting performance, January 2, 2011–January 31, 2014

| City | Model | RE (%) | UAPE (%) | MSPE (%) | MAPE (%) |
|---|---|---|---|---|---|
| Atlanta | Model 1 | −10.67 | 13.52 | 6.49 | 15.51 |
| | Model 2 | −8.99 | 12.96 | 5.99 | 14.73 |
| | Model 3 | −3.33 | 9.04 | 2.61 | 9.71 |
| | Model 4 | −3.42 | 9.05 | 2.62 | 9.73 |
| | Model 5 | −10.01 | 13.48 | 6.14 | 15.05 |
| | Model 6 | −3.17 | 9.03 | 2.58 | 9.71 |
| | Model 7 | −3.02 | 9.00 | 2.56 | 9.64 |
| Chicago | Model 1 | −26.68 | 26.89 | 49.18 | 45.60 |
| | Model 2 | −23.57 | 26.30 | 27.67 | 43.83 |
| | Model 3 | −6.95 | 20.22 | 17.30 | 24.88 |
| | Model 4 | −6.97 | 20.23 | 17.33 | 24.88 |
| | Model 5 | −25.74 | 26.41 | 36.21 | 44.98 |
| | Model 6 | −6.94 | 20.19 | 17.24 | 24.86 |
| | Model 7 | −6.92 | 18.88 | 17.18 | 24.64 |
| Dallas | Model 1 | −9.27 | 14.60 | 5.78 | 16.16 |
| | Model 2 | −9.06 | 14.33 | 4.11 | 14.98 |
| | Model 3 | −2.76 | 8.83 | 1.98 | 9.35 |
| | Model 4 | −2.92 | 8.83 | 2.00 | 9.36 |
| | Model 5 | −9.11 | 14.39 | 4.96 | 15.15 |
| | Model 6 | −2.64 | 8.80 | 1.96 | 9.34 |
| | Model 7 | −2.49 | 8.73 | 1.95 | 9.25 |
| New York | Model 1 | −11.46 | 15.93 | 9.95 | 18.75 |
| | Model 2 | −10.55 | 13.98 | 5.69 | 15.01 |
| | Model 3 | −4.01 | 9.98 | 3.84 | 10.93 |
| | Model 4 | −4.13 | 10.00 | 3.86 | 10.97 |
| | Model 5 | −10.74 | 14.98 | 6.48 | 16.65 |
| | Model 6 | −3.98 | 9.98 | 3.83 | 10.92 |
| | Model 7 | −3.89 | 9.89 | 3.80 | 10.90 |
| Philadelphia | Model 1 | −9.53 | 15.21 | 8.49 | 17.41 |
| | Model 2 | −7.19 | 14.60 | 7.61 | 16.40 |
| | Model 3 | −4.08 | 10.32 | 5.11 | 11.41 |
| | Model 4 | −4.21 | 10.34 | 5.13 | 11.44 |
| | Model 5 | −8.55 | 15.03 | 8.06 | 16.89 |
| | Model 6 | −4.06 | 10.32 | 5.09 | 11.40 |
| | Model 7 | −4.05 | 10.30 | 5.05 | 11.38 |
| Las Vegas | Model 1 | −2.20 | 9.34 | 1.40 | 9.55 |
| | Model 2 | −1.99 | 8.88 | 1.37 | 9.17 |
| | Model 3 | −0.44 | 5.02 | 0.40 | 5.09 |
| | Model 4 | −0.53 | 5.07 | 0.40 | 5.13 |
| | Model 5 | −2.05 | 9.15 | 1.38 | 9.28 |
| | Model 6 | −0.24 | 5.01 | 0.40 | 5.08 |
| | Model 7 | −0.23 | 4.98 | 0.37 | 5.02 |

Model 1 Alaton et al. (2002); Model 2 Huang et al. (2008); Model 3 Campbell and Diebold (2005); Model 4 Campbell and Diebold (2005) without controlling for seasonal effects in conditional volatility; Model 5 Benth and Saltyte-Benth (2007); Model 6 ARFIMA–GARCH process; Model 7 ARFIMA–SGARCH model, or Equations (2–6). RE, relative error; UAPE, unbiased absolute percentage error; MSPE, mean squared percentage error; and MAPE, mean absolute percentage error.

**TABLE 7** A 5-day ahead forecasting performance, January 2, 2011–January 31, 2014

| City | Model | RE (%) | UAPE (%) | MSPE (%) | MAPE (%) |
|---|---|---|---|---|---|
| Atlanta | Model 1 | −16.57 | 20.99 | 10.07 | 24.09 |
| | Model 2 | −13.96 | 20.13 | 9.31 | 22.88 |
| | Model 3 | −5.17 | 14.04 | 4.06 | 15.08 |
| | Model 4 | −5.30 | 14.05 | 4.07 | 15.11 |
| | Model 5 | −15.55 | 20.93 | 9.53 | 23.37 |
| | Model 6 | −4.92 | 14.02 | 4.01 | 15.07 |
| | Model 7 | −4.69 | 13.98 | 3.98 | 14.97 |
| Chicago | Model 1 | −41.43 | 41.76 | 76.38 | 70.82 |
| | Model 2 | −36.61 | 40.85 | 42.97 | 68.07 |
| | Model 3 | −10.80 | 31.40 | 26.87 | 38.64 |
| | Model 4 | −10.82 | 31.42 | 26.91 | 38.64 |
| | Model 5 | −39.97 | 41.02 | 56.24 | 69.85 |
| | Model 6 | −10.77 | 31.35 | 26.77 | 38.61 |
| | Model 7 | −10.75 | 29.32 | 26.67 | 38.26 |
| Dallas | Model 1 | −14.40 | 22.68 | 8.98 | 25.10 |
| | Model 2 | −14.07 | 22.26 | 6.38 | 23.26 |
| | Model 3 | −4.28 | 13.71 | 3.08 | 14.52 |
| | Model 4 | −4.53 | 13.72 | 3.10 | 14.53 |
| | Model 5 | −14.15 | 22.35 | 7.71 | 23.53 |
| | Model 6 | −4.09 | 13.67 | 3.05 | 14.51 |
| | Model 7 | −3.87 | 13.55 | 3.02 | 14.37 |
| New York | Model 1 | −17.79 | 24.73 | 15.46 | 29.12 |
| | Model 2 | −16.39 | 21.70 | 8.84 | 23.31 |
| | Model 3 | −6.22 | 15.50 | 5.96 | 16.98 |
| | Model 4 | −6.42 | 15.54 | 6.00 | 17.04 |
| | Model 5 | −16.68 | 23.26 | 10.06 | 25.86 |
| | Model 6 | −6.18 | 15.50 | 5.94 | 16.97 |
| | Model 7 | −6.04 | 15.37 | 5.91 | 16.93 |
| Philadelphia | Model 1 | −14.81 | 23.62 | 13.18 | 27.04 |
| | Model 2 | −11.17 | 22.67 | 11.81 | 25.48 |
| | Model 3 | −6.34 | 16.03 | 7.93 | 17.72 |
| | Model 4 | −6.53 | 16.06 | 7.97 | 17.77 |
| | Model 5 | −13.28 | 23.34 | 12.52 | 26.23 |
| | Model 6 | −6.30 | 16.03 | 7.91 | 17.71 |
| | Model 7 | −6.29 | 16.00 | 7.84 | 17.67 |
| Las Vegas | Model 1 | −3.42 | 14.51 | 2.17 | 14.83 |
| | Model 2 | −3.09 | 13.79 | 2.13 | 14.24 |
| | Model 3 | −0.68 | 7.80 | 0.63 | 7.91 |
| | Model 4 | −0.82 | 7.87 | 0.63 | 7.97 |
| | Model 5 | −3.18 | 14.21 | 2.14 | 14.41 |
| | Model 6 | −0.37 | 7.78 | 0.62 | 7.90 |
| | Model 7 | −0.36 | 7.74 | 0.58 | 7.79 |

Model 1 Alaton et al. (2002); Model 2 Huang et al. (2008); Model 3 Campbell and Diebold (2005); Model 4 Campbell and Diebold (2005) without controlling for seasonal effects in conditional volatility; Model 5 Benth and Saltyte-Benth (2007); Model 6 ARFIMA–GARCH process; Model 7 ARFIMA–SGARCH model, or Equations (2–6). RE, relative error; UAPE, unbiased absolute percentage error; MSPE, mean squared percentage error; and MAPE, mean absolute percentage error.

**TABLE 8** A 10-day ahead forecasting performance, January 2, 2011–January 31, 2014

| City | Model | RE (%) | UAPE (%) | MSPE (%) | MAPE (%) |
|---|---|---|---|---|---|
| Atlanta | Model 1 | −16.87 | 21.38 | 10.26 | 24.53 |
| | Model 2 | −14.22 | 20.51 | 9.48 | 23.30 |
| | Model 3 | −5.27 | 14.30 | 4.13 | 15.36 |
| | Model 4 | −5.40 | 14.31 | 4.15 | 15.39 |
| | Model 5 | −15.84 | 21.32 | 9.71 | 23.81 |
| | Model 6 | −5.01 | 14.28 | 4.08 | 15.35 |
| | Model 7 | −4.78 | 14.24 | 4.05 | 15.25 |
| Chicago | Model 1 | −42.20 | 42.53 | 77.80 | 72.13 |
| | Model 2 | −37.28 | 41.61 | 43.77 | 69.33 |
| | Model 3 | −11.00 | 31.98 | 27.36 | 39.35 |
| | Model 4 | −11.02 | 32.00 | 27.41 | 39.36 |
| | Model 5 | −40.71 | 41.78 | 57.28 | 71.14 |
| | Model 6 | −10.97 | 31.93 | 27.26 | 39.32 |
| | Model 7 | −10.95 | 29.86 | 27.17 | 38.97 |
| Dallas | Model 1 | −14.66 | 23.10 | 9.14 | 25.56 |
| | Model 2 | −14.33 | 22.67 | 6.50 | 23.69 |
| | Model 3 | −4.36 | 13.97 | 3.14 | 14.78 |
| | Model 4 | −4.61 | 13.97 | 3.16 | 14.80 |
| | Model 5 | −14.41 | 22.76 | 7.85 | 23.97 |
| | Model 6 | −4.17 | 13.92 | 3.10 | 14.78 |
| | Model 7 | −3.94 | 13.80 | 3.08 | 14.63 |
| New York | Model 1 | −18.12 | 25.19 | 15.74 | 29.66 |
| | Model 2 | −16.69 | 22.11 | 9.00 | 23.74 |
| | Model 3 | −6.34 | 15.78 | 6.07 | 17.29 |
| | Model 4 | −6.54 | 15.82 | 6.11 | 17.35 |
| | Model 5 | −16.99 | 23.69 | 10.24 | 26.34 |
| | Model 6 | −6.30 | 15.78 | 6.05 | 17.28 |
| | Model 7 | −6.15 | 15.65 | 6.02 | 17.24 |
| Philadelphia | Model 1 | −15.08 | 24.06 | 13.43 | 27.54 |
| | Model 2 | −11.37 | 23.09 | 12.03 | 25.95 |
| | Model 3 | −6.46 | 16.33 | 8.08 | 18.04 |
| | Model 4 | −6.65 | 16.35 | 8.11 | 18.09 |
| | Model 5 | −13.52 | 23.77 | 12.75 | 26.71 |
| | Model 6 | −6.42 | 16.33 | 8.05 | 18.04 |
| | Model 7 | −6.40 | 16.30 | 7.99 | 18.00 |
| Las Vegas | Model 1 | −3.48 | 14.78 | 2.21 | 15.11 |
| | Model 2 | −3.15 | 14.05 | 2.17 | 14.51 |
| | Model 3 | −0.70 | 7.94 | 0.64 | 8.06 |
| | Model 4 | −0.83 | 8.02 | 0.64 | 8.11 |
| | Model 5 | −3.24 | 14.47 | 2.18 | 14.67 |
| | Model 6 | −0.38 | 7.93 | 0.63 | 8.04 |
| | Model 7 | −0.37 | 7.88 | 0.59 | 7.93 |

Model 1 Alaton et al. (2002); Model 2 Huang et al. (2008); Model 3 Campbell and Diebold (2005); Model 4 Campbell and Diebold (2005) without controlling for seasonal effects in conditional volatility; Model 5 Benth and Saltyte-Benth (2007); Model 6 ARFIMA–GARCH process; Model 7 ARFIMA–SGARCH model, or Equations (2–6). RE, relative error; UAPE, unbiased absolute percentage error; MSPE, mean squared percentage error; and MAPE, mean absolute percentage error.

price of a contingent claim with a payoff $q_T$ at a future time $T$, denoted by $Y(t,T)$, then is

$$Y(t,T) = \frac{1}{U_c(\theta_t,t)} E_t(U_c(\theta_T,T)q_T) \ \forall t \in (0,T), \tag{11}$$

where $U_c(\theta_T,T)$ is the first derivative of the period- $T$ utility function on consumption, $c_T : U(c_T,T)$. Contingent claims on the temperature variable can be valued by Equation (11), as long as the temperature dynamics, dividend process, and the agent's preference determined by the relationship with the total consumption are specified first.

To value the temperature derivatives, an appropriate assumption for modeling temperature uncertainty should be considered. In light of the empirical results, the ARFIMA–SGARCH model provides empirical evidence of a dynamic process, using temperature data from different U.S. stations, as well as useful improvements in the fit and forecasting performance. Thus, we obtain an equilibrium valuation framework under the ARFIMA–SGARCH model, unlike Cao and Wei (2004). Other than the temperature dynamic, we assume that the agent's preference and the dividend process follow Cao and Wei (2004) setting, in which the representative investor has a risk preference characterized by constant relative risk aversion:

$$U(\theta_t,t) = e^{-\rho t} \frac{\theta_t^{\xi+1}}{\xi+1} \rho > 0, \ \xi \in (-\infty,0], \tag{12}$$

where $\rho$ is the rate of time preference, and $\xi$ is the risk parameter.

For the aggregate dividend process, Cao and Wei (2004) consider mean reversion in the rate of aggregate dividend change suggested Marsh and Merton (1987). The aggregate dividend model is as follows:

$$\ln \theta_t = a + \upsilon \ln \theta_{t-1} + \tau_t \ \forall \upsilon \leq 1, \text{ and} \tag{13}$$

$$\tau_t = \sigma\psi_t + \sigma\left[\frac{\lambda}{\sqrt{1-\lambda^2}}\varepsilon_t + \zeta_1\varepsilon_{t-1} + \zeta_2\varepsilon_{t-2} + \zeta_3\varepsilon_{t-3} + \ldots + \zeta_m\varepsilon_{t-m}\right], \ 0 \leq m \leq +\infty, \tag{14}$$

where $1-\upsilon$ is the speed of mean reversion, $\psi_t$ describes randomness due to all factors except for temperature, and $\varepsilon_t$ refers to innovations of the temperature variable defined in Equation (2). Thus the contemporaneous correlation between temperature and aggregate dividends is summarized in $\lambda$, and $\zeta_j$ is the coefficient of temperature-related lagged terms used to capture the lagged effects on aggregate dividend. Based on inevitability and assumption, $\sum_{j=1}^{m}\zeta_j^2(\forall m)$ is bounded. When $t$ represents a future time, the conditional variance of $\tau_t$ is $\sigma^2\left[1 + \frac{\lambda}{1-\lambda^2} + \sum_{j=1}^{m}\zeta_j^2\right]$, which can be explained in three parts: (1) all factors except for temperature contribute $\sigma^2$; (2) contemporaneous temperature contributes $\sigma^2\frac{\lambda}{1-\lambda^2}$; and (3) the lagged terms of the temperature contribute $\sigma^2\sum_{j=1}^{m}\zeta_j^2$. When $\lambda = 0$ and $\zeta_j = 0, \forall j$, the dividend process is independent of temperature innovations.

With the specification for the representative agent's preference in Equation (12), the dividend process in Equations (13) and (14), and the temperature dynamics in Equation (2–6) together with the equilibrium valuation framework in Equation (11), we can value a claim, contingent on the temperature variable.

## 4.2 | Valuation of HDD/CDD derivatives

Assume there is an HDD forward contract with a tick size of US $1, a strike price of $K$, and an accumulation of heating degree days between $T_1$ and $T_2$.[6] By applying Equations (11) and (12), we obtain the value at time $t$ of the HDD forward contracts,

$$\begin{aligned} f_{\text{HDD}}(t,T_1,T_2,K) &= E_t\left(\frac{U_c(\theta_{T_2},T_2)}{U_c(\theta_t,t)}[\text{HDD}(T_1,T_2) - K]\right) \\ &= e^{-\rho(T_2-t)}E_t\left(\frac{\theta_{T_2}^{\xi}}{\theta_t^{\xi}}[\text{HDD}(T_1,T_2) - K]\right) \end{aligned} \tag{15}$$

[6] $HDD(T_1,T_2)$ contract moths is November, December, January, February and March.

**TABLE 9** Base assumption of parameter values for pricing weather derivatives

| Parameter | Notion | Value | |
|---|---|---|---|
| Rate of time preference | $\rho$ | 3% | |
| Mean reversion[a] | $\upsilon$ | 0.9 | |
| S&P 500 daily return variance | $\sigma$ | 0.5381% | |
| Aggregative dividend lags | $m$ | 15 | |
| Risk aversion | $\xi$ | −2 | −10 |
| Contemporaneous correlation | $\lambda$ | 0.15 | 0.25 |
| Lags coefficient | $\zeta_j$ | $q^j\lambda$[b] | |

[a]The mean reversion rate is $1-\upsilon$.
[b]In the parameter, we follows Cao and Wei (2004) setup $\zeta_j = q^j\lambda$, $0 < q < 1$. The decay $q$ is chosen such that $q = \left(\frac{0.0001}{|\lambda|}\right)^{\frac{1}{30}}$.

By definition, the forward price at time $t$, $F_{\mathrm{HDD}}(t,T_1,T_2)$, is the value of $K$, which makes $f_{\mathrm{HDD}}(t,T_1,T_2,K) = 0$, so that

$$E_t\left(\frac{U_c(\theta_{T_2},T_2)}{U_c(\theta_t,t)}[\mathrm{HDD}(T_1,T_2)-K]\right) = 0. \tag{16}$$

In addition,

$$F_{\mathrm{HDD}}(t,T_1,T_2) = K = \frac{E_t[U_c(\theta_{T_2},T_2)\mathrm{HDD}(T_1,T_2)]}{E_t[U_c(\theta_{T_2},T_2)]} = \frac{E_t\left[\theta_{T_2}^{\xi}\mathrm{HDD}(T_1,T_2)\right]}{E_t\left[\theta_{T_2}^{\xi}\right]}. \tag{17}$$

Next, we consider a European HDD option with strike price $Z$ and denote the call and put prices at time $t$ as

$$C_{\mathrm{HDD}}(t,T_1,T_2,Z) = e^{-\rho(T_2-t)}\theta_t^{-\xi}E_t\left[\theta_{T_2}^{\xi}\max(\mathrm{HDD}(T_1,T_2)-Z,0)\right], \text{ and} \tag{18}$$

$$P_{\mathrm{HDD}}(t,T_1,T_2,Z) = e^{-\rho(T_2-t)}\theta_t^{-\xi}E_t\left[\theta_{T_2}^{\xi}\max(Z-\mathrm{HDD}(T_1,T_2),0)\right]. \tag{19}$$

The CDD derivatives analogously can be expressed by replacing HDD with CDD notations. Using the valuation framework in Equations (17–19), we decompose the derivative price into the expected future spot value and the market price of risk (i.e., risk premium). With HDD forward contracts as an example, we clarify the relationship between the value and the risk premium as follows.

$$\begin{aligned} F_{\mathrm{HDD}}(t,T_1,T_2) &= \frac{E_t\left[\theta_{T_2}^{\xi}\mathrm{HDD}(T_1,T_2)\right]}{E_t\left[\theta_{T_2}^{\xi}\right]} \\ &= \frac{\mathrm{Cov}\left(\theta_{T_2}^{\xi},\mathrm{HDD}(T_1,T_2)\right) + E_t\left[\theta_{T_2}^{\xi}\right]E_t[\mathrm{HDD}(T_1,T_2)]}{E_t\left[\theta_{T_2}^{\xi}\right]} \\ &= E_t[\mathrm{HDD}(T_1,T_2)] + \frac{\mathrm{Cov}\left(\theta_{T_2}^{\xi},\mathrm{HDD}(T_1,T_2)\right)}{E_t\left[\theta_{T_2}^{\xi}\right]} \\ &= E_t[\mathrm{HDD}(T_1,T_2)] + \Psi_{F,\mathrm{HDD}}(T_2) \end{aligned}, \tag{20}$$

where Cov(•) indicates covariance, the first term represents the expected future spot value of HDD, and the second term represents the forward premium. The formula for the CDD derivative can be obtained similarly. Because of the negative correlation between HDD and temperature, the risk premium in Equation (20) is negative; it is positive for the CDD derivatives. Therefore, we can discover the risk premium for different temperature derivatives. We use Monte Carlo simulations to calculate the price for temperature derivatives and analyze the corresponding numerical results next.

**TABLE 10** Risk premium in HDD forward contracts

| | | $\xi = -2$ | | $\xi = -10$ | |
|---|---|---|---|---|---|
| **City** | **Risk-neutral forward** | $\lambda = -0.15$ (%) | $\lambda = 0.15$ (%) | $\lambda = -0.15$ (%) | $\lambda = 0.15$ (%) |
| Atlanta | 1912.2 | 1.27 | −1.23 | 3.11 | −3.17 |
| Chicago | 2733.5 | 1.78 | −1.61 | 4.02 | −4.35 |
| Dallas | 2485.4 | 1.24 | −1.17 | 2.89 | −3.10 |
| New York | 2450.1 | 1.69 | −1.58 | 3.87 | −4.09 |
| Philadelphia | 2182.2 | 1.98 | −1.84 | 4.51 | −4.81 |
| Las Vegas | 1367.6 | 2.14 | −1.97 | 4.71 | −5.01 |
| | | $\lambda = -0.25$ (%) | $\lambda = 0.25$ (%) | $\lambda = -0.25$ (%) | $\lambda = 0.25$ (%) |
| Atlanta | 1912.2 | 1.89 | −1.78 | 3.28 | −3.41 |
| Chicago | 2733.5 | 2.11 | −2.25 | 5.14 | −5.71 |
| Dallas | 2485.4 | 1.76 | −1.67 | 3.15 | −3.88 |
| New York | 2450.1 | 2.01 | −2.09 | 4.99 | −5.41 |
| Philadelphia | 2182.2 | 2.41 | −2.51 | 5.48 | −5.91 |
| Las Vegas | 1367.6 | 2.89 | −2.72 | 5.99 | −6.14 |

The risk-neutral forward contract is calculated by $\lambda = 0, \xi_j = 0, \forall i$. Other entries are the percentage differences between the risk-neutral value and the forward price.

**TABLE 11** Risk premium in HDD option

| | | | $\xi = -2$ | | $\xi = -10$ | |
|---|---|---|---|---|---|---|
| **City** | **Contract** | **Risk-neutral price** | $\lambda = -0.15$ (%) | $\lambda = 0.15$ (%) | $\lambda = -0.15$ (%) | $\lambda = 0.15$ (%) |
| Atlanta | Call | 50.270 | 2.35 | −2.15 | 10.04 | −11.49 |
| | Put | 50.270 | −2.14 | 2.04 | −9.79 | 10.25 |
| Chicago | Call | 56.270 | 2.97 | −3.01 | 11.81 | −12.89 |
| | Put | 56.270 | −2.81 | 2.75 | −10.41 | 12.98 |
| Dallas | Call | 47.623 | 2.29 | −2.01 | 9.89 | −10.10 |
| | Put | 47.623 | −1.87 | 1.96 | −9.14 | 9.58 |
| New York | Call | 43.998 | 2.85 | −2.47 | 10.99 | −12.14 |
| | Put | 43.998 | −2.57 | 2.58 | −10.08 | 12.58 |
| Philadelphia | Call | 50.436 | 3.18 | −3.24 | 12.04 | −13.90 |
| | Put | 50.436 | −2.98 | 2.95 | −10.57 | 13.04 |
| Las Vegas | Call | 50.705 | 3.98 | −3.78 | 13.01 | −14.25 |
| | Put | 50.705 | −3.77 | 3.58 | −11.78 | 14.54 |
| | | | $\lambda = -0.25$ (%) | $\lambda = 0.25$ (%) | $\lambda = -0.25$ (%) | $\lambda = 0.25$ (%) |
| Atlanta | Call | 50.270 | 2.61 | −2.70 | 11.12 | −12.81 |
| | Put | 50.270 | −2.58 | 2.35 | −10.87 | 11.87 |
| Chicago | Call | 56.270 | 3.14 | −3.78 | 12.41 | −13.54 |
| | Put | 56.270 | −3.55 | 3.58 | −11.97 | 13.85 |
| Dallas | Call | 47.623 | 2.58 | −2.45 | 10.81 | −11.45 |
| | Put | 47.623 | −2.73 | 2.14 | −9.58 | 10.55 |
| New York | Call | 43.998 | 3.08 | −3.62 | 11.58 | −12.94 |
| | Put | 43.998 | −3.28 | 3.42 | −11.01 | 12.97 |
| Philadelphia | Call | 50.436 | 3.52 | −3.82 | 13.04 | −14.02 |
| | Put | 50.436 | −4.02 | 4.12 | −12.41 | 14.91 |
| Las Vegas | Call | 50.705 | 4.02 | −4.34 | 14.58 | −15.04 |
| | Put | 50.705 | −4.92 | 4.98 | −15.28 | 15.87 |

If the risk-neutral call and put options were at-the-money and equality, under the ARFIMA–SGARCH price process, we would set the strike price equal to the risk-neutral forward price. Other entries are the percentage differences between the risk-neutral value and the option contract.

**TABLE 12** Model risk for pricing HDD weather derivatives

| City | Temperature pattern | Forward (%) | Option (%) |
|---|---|---|---|
| Atlanta | Ignoring seasonal cycles in mean | 11.50 | 20.47 |
| | Ignoring global warming | 4.48 | 9.57 |
| | Ignoring cyclical components in mean | 19.51 | 48.14 |
| | Ignoring long memory | 9.87 | 14.87 |
| | Ignoring seasonal cycles in volatility | 5.99 | 13.41 |
| | Ignoring volatility clustering | 11.92 | 30.14 |
| Chicago | Ignoring seasonal cycles in mean | 10.51 | 19.11 |
| | Ignoring global warming | 4.18 | 6.13 |
| | Ignoring cyclical components in mean | 15.13 | 45.55 |
| | Ignoring long memory | 9.75 | 14.56 |
| | Ignoring seasonal cycles in volatility | 5.19 | 12.82 |
| | Ignoring volatility clustering | 11.19 | 29.87 |
| Dallas | Ignoring seasonal cycles in mean | 10.87 | 19.84 |
| | Ignoring global warming | 3.12 | 4.76 |
| | Ignoring cyclical components in mean | 18.12 | 46.58 |
| | Ignoring long memory | 8.74 | 12.97 |
| | Ignoring seasonal cycles in volatility | 4.94 | 11.59 |
| | Ignoring volatility clustering | 10.19 | 28.79 |
| New York | Ignoring seasonal cycles in mean | 12.51 | 20.18 |
| | Ignoring global warming | 5.14 | 7.39 |
| | Ignoring cyclical components in mean | 17.89 | 47.81 |
| | Ignoring long memory | 10.59 | 15.81 |
| | Ignoring seasonal cycles in volatility | 7.01 | 13.54 |
| | Ignoring volatility clustering | 13.17 | 34.81 |
| Philadelphia | Ignoring seasonal cycles in mean | 12.54 | 21.98 |
| | Ignoring global warming | 4.99 | 9.68 |
| | Ignoring cyclical components in mean | 20.14 | 49.97 |
| | Ignoring long memory | 10.28 | 15.29 |
| | Ignoring seasonal cycles in volatility | 6.74 | 14.58 |
| | Ignoring volatility clustering | 12.78 | 32.84 |
| Las Vegas | Ignoring seasonal cycles in mean | 11.53 | 20.01 |
| | Ignoring global warming | 3.81 | 5.91 |
| | Ignoring cyclical components in mean | 19.58 | 47.81 |
| | Ignoring long memory | 9.21 | 13.49 |
| | Ignoring seasonal cycles in volatility | 5.42 | 12.14 |
| | Ignoring volatility clustering | 13.29 | 29.14 |

The risk-neutral forward contract is calculated by $\lambda = 0, \xi_j = 0, \forall i$. Model risk is the percentage difference between the ARFIMA–SGARCH model and a model that ignores temperature properties in a risk-neutral setting.

## 4.3 | Simulation and analysis

We analyze the price of temperature derivatives in this subsection, to discover the model risk by pricing temperature derivatives numerically. Table 9 contains the base parameter values we used to calculate the price of HDD and CDD forward and option contracts. For comparison purposes, we set the parameters of the equilibrium approach with the same assumptions adopted by Cao and Wei (2004). Because by nature HDD contracts are mirror images of CDD contracts, we only report the results for the

HDD contracts in the period from November 1, 2013 to March 31, 2014 and the values of HDD derivative are calculated as the 500,000 sample paths by the software Matlab 7.10.

We first investigate the risk premiums for HDD contracts. According to the definition of risk premium ($\Psi$) in Equation (20), we present the effect of the risk premium by calculating the percentage difference between the derivative values and the risk-neutral value for each derivative. Tables 10 and 11 shows the simulated results of HDD forward and option contract prices under the ARFIMA–SGARCH model for all six cities separately. The risk premium in different cities varies, but the effects on the risk premium are in line with Cao and Wei (2004). For example, the correlation's sign determines the sign of the risk premium. Given a fixed correlation, greater risk aversion requires a larger risk premium, so it makes sense that investors ask for higher returns. At the same risk aversion level, a closer correlation leads to a larger risk premium. Risk premiums for option contracts are larger than those for forward contracts, because of their different payoff types, that is, linear versus non-linear.

The advantage of the proposed ARFIMA Seasonal GARCH model is that it allows for long memory effects as well as other important temperature properties that govern temperature dynamics. In turn, we can discover model risk and its effect on the price of temperature derivatives. To investigate model risk, we calculate the HDD forward and option contract prices, ignoring some temperature properties,[7] as we indicate in Table 12. The effects of model risk for the six cities are consistent. First, ignoring any temperature feature leads to underestimates of the HDD forward and option contract prices—such as 8.74–10.59% and 12.97–15.81% underestimates of model risk in forward and option contracts, respectively, when using the temperature model proposed by Campbell and Diebold (2005) and thus ignoring the long memory property in temperature. Second, model risk is very significant, ranging from 3.12 to 20.14% and 4.76 to 49.97% for forward and option contracts, respectively. Third, the most significant model risk stems from ignoring the cyclical components in mean; the least significant involves ignoring global warming. The empirical results are consistent with Jewson and Brix (2005), they conclude small misspecification in the models can lead to large mispricing of the temperature contract. Fourth, the model risk for options is more significant than that for forward contracts, because of their distinct payoff types. Therefore, it is important to understand temperature behavior and consider appropriate temperature models when pricing weather derivatives.

## 5 | CONCLUSIONS

Managing weather risk has become more important in the modern environment of climate change. Modeling weather dynamics also is crucial to the valuation of weather derivatives. This article investigates temperature behavior and proposes a ARFIMA–SGARCH model that allows for the long memory effect and other temperature properties addressed in existing literature. That is, it considers seasonal effects, cyclical components, global warming, long memory in the conditional mean and seasonal effect, and cyclical components in conditional variance. With data from six illustrative cities (Atlanta, Chicago, Dallas, New York, Philadelphia, and Las Vegas), our empirical study confirms that the ARFIMA–SGARCH model matches evidence of temperature dynamic processes and provides useful improvements in fit and forecasting performance. Therefore, existing temperature models that consider long memory effects but ignore other temperature properties cannot capture temperature dynamics.

Because the underlying temperature variable is not tradable and the market is incomplete, to apply our proposed ARFIMA–SGARCH model for pricing temperature derivatives, we built an equilibrium option pricing framework for HDD and CDD forward and option contracts, such that we studied the impact of model risk on pricing HDD and CDD forward and option contracts numerically. Model risk for pricing the temperature derivative is significant when we ignore any temperature property.

Finally, in the light of our analysis, a comparison of temperature modeling and forecasting between the daily modeling approach with index approach is worth investigating due to most practitioners rely on the index modeling framework since it is easy to understand (Davis 2001; Dorfleitner & Wimmer 2010; Jewson & Brix, 2005). On the other hand, another important issue for pricing is that there is still no consensus about the best way to price weather derivatives due to weather cannot to be traded. Therefore, the comparison of different pricing approach is an interesting issue for weather derivatives. The study of temperature behavior and the valuation framework applied under the different approach will provide deep insights for encouraging the development of the weather derivative market.

[7]Due to the ARFIMA–SGARCH is the complex model, we can use the different coefficients setup to discover model risk. For example, we can set the parameter $\hat{d} = 0$ if we ignore the long memory effect and we can set $\alpha_i = 0$ if we ignore the global warming properties.

## ORCID

*Jr-Wei Huang* http://orcid.org/0000-0002-1149-4507

## REFERENCES


Akaike, H. (1973). *Information theory and an extension of the maximum likelihood principle* (2nd ed., pp. 267–281). Budapest, Hungary: Akadémiai Kiadó.

Alaton, P., Djehiche, B., & Dtillberger, D. (2002). On modelling and pricing weather derivatives. *Applied Mathematical Finance*, *9*, 1–20.

Aydogan, K., & Booth, G. C. (1988). Are there long cycles in common stock returns? *Southern Economic Journal*, *55*, 141–149.

Baillie, R. T. (1996). Long memory process and fractional integration in econometrics. *Journal of Econometrics*, *73*, 5–59.

Benth, F. E. (2003). On arbitrage-free pricing of weather derivatives based on fractional brownian motion. *Applied Mathematical Finance*, *10*, 303–324.

Benth, F. E., & Saltyte-Benth, J. (2007). The volatility of temperature and pricing of weather derivatives. *Quantitative Finance*, *7*, 553–561.

Brockett, P. L., Wang, M., & Yang, C. (2005). Weather derivatives and weather risk management. *Risk Management and Insurance Review*, *8*, 127–140.

Brody, D. C., Syroka, J., & Zervos, M. (2002). Dynamical pricing of weather derivatives. *Quantitative Finance*, *2*, 189–198.

Caballero, R., Jewson, S., & Zervos, M. (2002). Long memory in surface air temperature: detection, modelling and application to weather derivative valuation. *Climate Research*, *21*, 127–140.

Campbell, S. D., & Diebold, F. X. (2005). Weather forecasting for weather derivatives. *Journal of the American Statistical Association*, *100*, 6–16.

Cao, M., & Wei, J. (2004). Weather derivatives valuation and market price of weather risk. *Journal of Futures Markets*, *24*, 1065–1089.

Cheung, Y. W. (1993). Long memory in foreign exchange rates. *Journal of Business and Economics Statistics*, *11*, 93–101.

Cheung, Y., & Lai, K. (1995). A search for long memory in international stock market returns. *Journal of International Money and Finance*, *14*, 597–615.

Chow, K. V., Denning, K. C., Ferris, S., & Noronha, G. (1995). Long-term and short-term price memory in the stock market. *Economics Letters*, *49*, 287–295.

Davis, M. (2001). Pricing weather derivatives by marginal value. *Quantitative Finance*, *1*, 1–4.

Dickey, D., & Fuller, W. A. (1981). Likelihood ratio statistic for autoregressive time series with a unit root. *Econometrica*, *49*, 1057–1072.

Dorfleitner, G., & Wimmer, M. (2010). The pricing of temperature futures at the Chicago Mercantile Exchange. *Journal of Banking and Finance*, *34*, 1360–1370.

Geweke, J., & Porter-Hudak, S. (1983). The estimation and application of long memory time series models. *Journal of Time Series Analysis*, *4*, 221–238.

Granger, C. W. J., & Joyeux, R. (1980). An introduction to long-memory series models and fractional differencing. *Journal of Time Series Analysis*, *1*, 15–30.

Greene, M. T., & Fielitz, B. D. (1977). Long-term dependence in common stock returns. *Journal of Financial Economics*, *5*, 339–349.

Groll, A., Brenda, L., & Meyer-Brandis, T. (2016). A consistent two-factor model for pricing temperature derivatives. *Energy Economics*, *55*, 112–126.

Hardle, W. K., & Lopez Cabrera, B. (2012). The implied market price of weather risk. *Applied Mathematical Finance*, *19*, 59–95.

Hosking, J. R. M. (1981). Fractional differencing. *Biometrika*, *68*, 165–176.

Huang, H. H., Shiu, Y. M., & Lin, P. S. (2008). HDD and CDD option pricing with market price of weather risk for Taiwan. *Journal of Futures Markets*, *28*, 790–814.

Hurst, H. (1951). Long term storage capacity of reservoirs. *Transactions of the American Society of Civil Engineers*, *116*, 770–799.

Impact Forecasting. (2013). *November 2013 global catastrophe recap*. Retrieved from http://thoughtleadership.aonbenfield.com/Documents/20131205_if_november_global_recap.pdf

Intergovernmental Panel on Climate Change (IPCC). (2008). *Climate change and water* (Technical Paper, IPCC, 6). Retrieved from http://www.ipcc.ch/pdf/technical-papers/climate-change-water-en.pdf

Jacobsen, B. (1996). Long term dependence in stock returns. *Journal of Empirical Finance*, *3*, 393–417.

Jewson, S., & Brix, A. (2005). *Weather derivative valuation: The meteorological, Statistical, financial and mathematical foundations*. New York: Cambridge University Press.

Jewson, S., & Caballero, R. (2003). Seasonality in the statistics of surface air temperature and the pricing of weather derivatives. *Meteorological Applications*, *10*, 367–376.

Ling, S., & Li, W. K. (1997). On fractionally integrated autoregressive moving-average time series models with conditional heteroscedasticity. *Journal of the American Statistical Association*, *92*, 1184–1194.

Lo, A. W. (1991). Long-term memory in stock market prices. *Econometrica*, *59*, 1279–1313.

Lobell, D. B., Ortiz-Monasterio, J. I., & Falcon, W. P. (2007). Yield uncertainty at the field scale evaluated with multi-year satellite data. *Agricultural Systems*, *92*, 76–90.

Lucas, R. E. (1978). Asset prices in an exchange economy. *Econometrica*, *46*, 1429–1445.

Marsh, T. A., & Merton, R. (1987). Dividend behavior for the aggregate stock market. *Journal of Business*, *60*, 1–40.

Neese, J. M. (1994). Systematic biases in manual observations of maximum and minimum temperature. *Journal of Climate*, *7*, 834–842.

Papazian, G., & Skiadopoulos, G. (2010). *Modeling the dynamics of temperature with a view to weather derivatives* (Working Paper). Retrieved from https://ssrn.com/abstract=1517293 or https://doi.org/10.2139/ssrn.1517293

Phillips, P., & Perron, P. (1988). Testing for a unit root in time series regression. *Biometrica*, *75*, 335–346.

Schiller, F., Seidler, G., & Wimmer, M. (2012). Temperature models for pricing weather derivatives. *Quantitative Finance*, *12*, 489–500.

Syroka, J., & Toumi, R. (2001). Scaling and persistence in observed and modelled surface temperature. *Geophysical Research Letter*, *28*, 3255–3258.

Tsonis, A. A., Roebber, P. J., & Elsner, J. B. (1999). Long-range correlations in the extratropical atmospheric circulation: Origins and implications. *Journal of Climate*, *12*, 1534–1541.

Weather Risk Management Association. (2011a). *Weather derivatives market shows robust growth in 2010–2011*. Retrieved from http://web.archive.org/web/20131203203136/ http://www.wrma.org/pdf/WRMA2011IndustrySurveypressreleaseFINAL.pdf

Weather Risk Management Association. (2011b). *Weather risk derivative survey prepared for the weather risk management association*. Retrieved from http://files.ctctcdn.com/6ae11b18001/9c748764-22ad-4898-ba75-a3353c5859ce.pdf

Zapranis, A., & Alexandridis, A. (2009). Weather derivatives pricing: Modeling the seasonal residual variance of an Ornstein-Uhlenbeck temperature process with neural networks. *Neurocomputing*, *73*, 37–48.

**How to cite this article:** Huang J-W, Yang SS, Chang C-C. Modeling temperature behaviors: Application to weather derivative valuation. *J Futures Markets*. 2018;38:1152–1175. https://doi.org/10.1002/fut.21923

## APPENDIX A

We use an econometric approach to detect the potential presence of long memory in temperature, with three methods introduced by Hurst (1951), Lo (1991), and Geweke and Porter-Hudak (1983).

### Hurst (1951)

Let $W_t$ denote the temperature at time $t$ and define $X_t = \ln(W_t) - \ln(W_{t-1})$ to be the rate of change for the temperature from $t-1$ to $t$. Hurst (1951) defines the rescaled range (R/S) statistic as follows:

$$R/S = \frac{1}{\left[\frac{1}{N}\sum_{j=1}^{N}\left(X_j - \bar{X}_N\right)^2\right]^{1/2}} \times \left[\max_{1\le k\le N}\sum_{j=1}^{k}\left(X_j - \bar{X}_N\right) - \min_{1\le k\le N}\sum_{j=1}^{k}\left(X_j - \bar{X}_N\right)\right], \tag{A.1}$$

where $N$ is the number of observations, and $\bar{X} = \frac{1}{N}\sum_{j=1}^{N} X_j$. To obtain the Hurst exponent we use the following formula:

$$H \sim \frac{\log(R/S)}{\log(N)},\ 0 < H < 1, \tag{A.2}$$

where $H$ refers to the Hurst exponent, such that for $0.5 < H < 1$, the process has a long memory;[8] for $0 < H < 0.5$, it is anti-persistent;[9] and for $H = 0.5$, it has a short memory.

### Lo (1991)

Lo notes that the R/S statistic misbehaved in the presence of short memory; that is, it tends to be high and suggests a long memory, even when the time series contains only short memory. Lo (1991) suggests a modified R/S statistic that is sensitive to the long memory but not the short memory, as well as a significance test for R/S, defined as

$$R/S(q) = \frac{1}{\hat{\sigma}_N(q)} \times \left[\max_{1\le k\le N}\sum_{j=1}^{k}\left(X_j - \bar{X}_N\right) - \min_{1\le k\le N}\sum_{j=1}^{k}\left(X_j - \bar{X}_N\right)\right], \tag{A.3}$$

[8]The autocorrelations are all positive and decay at a hyperbolic rate.

[9]The anti-persistent state is a long memory effect, because its autocorrelations are negative and decay hyperbolically to zero (Baillie, 1996).

$$\hat{\sigma}_N^2(q) = \frac{1}{N}\sum_{j=1}^{N}\left(X_j - \bar{X}_N\right)^2 + \frac{2}{N}\sum_{j=1}^{q} w_j(q)\left\{\sum_{i=j+1}^{N}\left(X_i - \bar{X}_N\right)\left(X_{i-j} - \bar{X}_N\right)\right\}, \tag{A.4}$$

$$w_j(q) = 1 - \frac{j}{q+1},\ q < N, \text{ and} \tag{A.5}$$

$$q = [k_N],\ k_N = \left(\frac{3N}{2}\right)^{\frac{1}{3}} \cdot \left(\frac{2\hat{\rho}}{1-\hat{\rho}^2}\right)^{\frac{2}{3}}, \tag{A.6}$$

where $[k_N]$ denotes the greatest integer less than or equal to $k_N$, and $\hat{\rho}$ is the estimated first-order autocorrelation coefficient of the data. For the significance test, we must compute the following statistic:

$$V = \frac{R/S(q)}{\sqrt{N}}. \tag{A.7}$$

We compare it against the critical values provided by Lo (1991): 1.747 at the 5% level and 1.620 at the 10% level.

**Geweke and Porter-Hudak (1983)**

Geweke and Porter-Hudak (1983) were the first to suggest a log-periodogram regression to estimate the fractional differencing parameter $d$. Let $I(w_j)$ be the sample periodogram at the $j$th Fourier frequency $w_j = 2\pi j/N$ ($j = 1, ..., [N/2]$). The estimate can be obtained from the following regression, estimated by least squares:

$$\ln(I(w_j)) = c - 2d\ln(2\sin(w_j/2)) + \varepsilon_j. \tag{A.8}$$

Using observations pertaining to frequencies ranging from $j = 1$ to $m$, $m$ acts as an upper bound on the number of frequencies used. A popular rule of thumb is $m = N^{1/2}$. As a matter of notation, let

$$\begin{aligned} a_j &= -\ln(2\sin(w_j/2)) + \frac{1}{m}\sum_{k=1}^{m}\ln(2\sin(w_k/2)) \\ &= -\ln\left|1 - \exp(iw_j)\right| + \frac{1}{m}\ln|1 - \exp(iw_k)| \end{aligned}, \tag{A.9}$$

and $S_N = \sum_{k=1}^{m} a_j^2$. The estimate of $d$ is then

$$\hat{d} = \frac{1}{2S_N}\sum_{j=1}^{m} a_j \ln\left(I(w_j)\right). \tag{A.10}$$

The $a_j$ are demeaned values of the regressors that sum to zero; in addition, $m^{-1}S_N \to 1$ as $N \to \infty$. Its distribution is as follows:

$$\hat{d} \sim N\left(d, \pi^2\left[6\sum_{j=1}^{m}\left(V_j - \bar{V}\right)^2\right]^{-1}\right), \tag{A.11}$$

where $V_j = -2\ln(w_j)$ and $\bar{V} = \frac{1}{m}\sum_{j=1}^{m} V_j$. This result provides a significant test of $\hat{d}$, in which $\hat{d}$ refers to the fractional differencing parameter, where if $0 < \hat{d} < 0.5$, the process has a long memory; if $-0.5 < \hat{d} < 0$, the process is anti-persistent; if $\hat{d} = 0$, the process has a short memory (e.g., ARMA process); and if $\hat{d} = 1$, it turns into a non-stationary process (e.g., ARIMA).

## APPENDIX B

We briefly introduce various temperature models.

**Alaton et al. (2002) Model 1**

Alaton et al. (2002) propose a temperature model to describe the daily average temperature at time $t$:

$$W_t = \iota_0 + \iota_1 t + \iota_2 \sin wt + \iota_3 \cos wt + \eta_t, \eta_t \sim \mathrm{IID}\left(0, \sigma^2\right), \tag{B.1}$$

The Equation (B.1) is formulated on the basis of two assumptions: (1) The trend of the gentle increase in temperature is linear; and (2) seasonality can be captured in a sine function. The parameters $(\iota_0, \iota_1, \iota_2, \iota_3)$ are estimated using ordinary least squares regressions. The constant variance assumption relies on month-specific variances.

**Huang et al. (2008) Model 2**

Huang et al. (2008) extend the model by Alaton et al. (2002) by relaxing the assumption that $\eta_t$ is autocorrelated. Assume $\eta_t$ follows a GARCH process. Equation (B.1) can be rewritten as:

$$\begin{aligned} W_t &= \iota_0 + \iota_1 t + \iota_2 \sin wt + \iota_3 \cos wt + \eta_t,\ \eta_t | F_{t-1} \sim N\left(0, \sigma_t^2\right) \\ \sigma_t^2 &= \phi_0 + \sum_{i=1}^{p} \phi_1 \eta_{t-i}^2 + \sum_{j=1}^{q} \phi_2 \sigma_{t-i}^2 \end{aligned} . \tag{B.2}$$

They use the GARCH process to capture conditional variance, which also displays strong cyclical persistence.

**Campbell and Diebold (2005) Model 3**

Campbell and Diebold (2005) focus on conditional mean dynamics, with contributions from global warming and seasonal and cyclical components, together with conditional variance, with contributions from both seasonal and cyclical components. The daily average temperature model is as follows:

$$W_t = \mathrm{Trend}_t + \mathrm{Seasonal}_t + \sum_{l=1}^{L} \rho_{t-l} W_{t-1} + \sigma_t \varepsilon_r, \tag{B.3}$$

$$\begin{aligned} \mathrm{Trend}_t &= \beta_1 t \\ \mathrm{Seasonal}_t &= \sum_{p=1}^{p} \left( \sigma_{c,p} \cos\left(\frac{2\pi\ \mathrm{pt}}{365}\right) + \sigma_{s,p} \sin\left(\frac{2\pi\ \mathrm{pt}}{365}\right) \right), \end{aligned}$$

where

$$\begin{aligned} \sigma_t^2 &= \sum_{q=1}^{Q} \left( \gamma_{c,q} \cos\left(\frac{2\pi\ \mathrm{qt}}{365}\right) + \gamma_{s,q} \sin\left(\frac{2\pi\ \mathrm{qt}}{365}\right) \right) + \sum_{r=1}^{R} \alpha_r \left(\sigma_{t-r} \varepsilon_{t-r}\right)^2 + \sum_{s=1}^{S} \beta_s \sigma_{t-s}^2 \\ \varepsilon_t &\sim \mathrm{iidN}(0, 1) \end{aligned} \tag{B.4}$$

**Campbell and Diebold (2005) with standard GARCH, Model 4**

Model 4 relies on Campbell and Diebold (2005) methodology; time-varying volatility is a GARCH process of Equation (B.4), rewritten as follows:

$$\sigma_t^2 = \phi_0 + \sum_{r=1}^{R} \alpha_r \left(\sigma_{t-r} \varepsilon_{t-r}\right)^2 + \sum_{s=1}^{S} \beta_s \sigma_{t-s}^2. \tag{B.5}$$

Comparing Models 3 and 4 reveals the difference in fit and forecasting performance when we ignore seasonal variation in the conditional variance effect for average temperature dynamics.

**Benth and Saltyte-Benth (2007), Model 5**

Model 5 relies on Benth and Saltyte-Benth (2007) models, they propose the following Ornstein–Uhlenbeck model for the time evolution of temperature:

$$dW_t = ds_t - \kappa(W_t - S_t)dt + \sigma_t dB_t \tag{B.6}$$

where

$$\begin{aligned} s_t &= a + bt + \sum_{i=1}^{I_1} a_i \sin(2i\pi(t - f_i)/365) + \sum_{j=1}^{J_1} b_j \cos(2j\pi(t - g_i)/365), \\ \sigma_t^2 &= c + \sum_{i=1}^{I_2} c_i \sin(2i\pi t/365) + \sum_{j=1}^{J_2} d_j \cos(2j\pi t/365) \end{aligned} \tag{B.7}$$

**ARFIMA–GARCH Model 6**

Model 6 reports the estimated temperature on the basis of the ARFIMA–GARCH model, without controlling for seasonal variation in conditional variance. Thus the average temperature in period $t$ is given as:

$$W_t = u_t + \varepsilon_t,$$

where

$$u_t = \alpha_0 + \alpha_1 t + \sum_{j=1}^{P} \left( \delta_j \cos\left(\frac{2jt\pi}{365}\right) + \gamma_l \sin\left(\frac{2jt\pi}{365}\right) \right).$$

The stochastic component of the daily average temperature $\varepsilon_t$ follows a ARFIMA–GARCH model:

$$\begin{aligned} \Phi(L)(1 - L)^d \varepsilon_t &= \Theta(L)\eta_t, \\ \eta_t | F_{t-1} &\sim N\left(0, h_t^2\right), \text{ and} \\ h_t^2 &= \phi_0 + \sum_{j=1}^{Q} \omega_j \eta_{t-j}^2 + \sum_{i=1}^{E} \beta_i h_{t-i}^2. \end{aligned} \tag{B.8}$$

**ARFIMA–SGARCH, Model 7**

Model 7 is the ARFIMA–SGARCH methodology described by Equations (2–6) in section 3.1.